DEBRIS FLOWS: Disasters, Risk, Forecast, Protection

Proceedings
of the 5th International Conference

Tbilisi, Georgia, 1-5 October 2018

Editors
S.S. Chernomorets, G.V. Gavardashvili

Publishing House "Universal"
Tbilisi 2018

СЕЛЕВЫЕ ПОТОКИ: катастрофы, риск, прогноз, защита

Труды
5-й Международной конференции

Тбилиси, Грузия, 1-5 октября 2018 г.

Ответственные редакторы
С.С. Черноморец, Г.В. Гавардашвили

Издательство Универсал
Тбилиси 2018

ღვარცოფები:
კატასტროფები, რისკი, პროგნოზი, დაცვა

მე–5 საერთაშორისო კონფერენციის
მასალები

თბილისი, საქართველო, 1–5 ოქტომბერი, 2018

რედაქტორები
ს.ს. ჩერნომორეც, გ.ვ. გავარდაშვილი

გამომცემლობა "უნივერსალი"
თბილისი 2018

УДК 551.311.8
ББК 26.823

Селевые потоки: катастрофы, риск, прогноз, защита. Труды 5-й Международной конференции. Тбилиси, Грузия, 1-5 октября 2018 г. – Отв. ред. С.С. Черноморец, Г.В. Гавардашвили. – Тбилиси: Универсал, 2018, 671 с.

Debris Flows: Disasters, Risk, Forecast, Protection. Proceedings of the 5th International Conference. Tbilisi, Georgia, 1-5 October 2018. – Ed. by S.S. Chernomorets, G.V. Gavardashvili. – Tbilisi: Publishing House "Universal", 2018, 671 p.

ღვარცოფები: კატასტროფები, რისკი, პროგნოზი, დაცვა. მე–5 საერთაშორისო კონფერენციის მასალები. თბილისი, საქართველო, 1–5 ოქტომბერი, 2018. გამომცემლობა "უნივერსალი", თბილისი 2018, 671 გვ. პასუხისმგებელი რედაქტორები ს.ს. ჩერნომორეც, გ.ვ. გავარდაშვილი.

Ответственные редакторы С.С. Черноморец, Г.В. Гавардашвили
Edited by S.S. Chernomorets, G.V. Gavardashvili

Верстка: С.С. Черноморец, К.С. Висхаджиева, Е.А. Савернюк
Page-proofs: S.S. Chernomorets, K.S. Viskhadzhieva, E.A. Savernyuk

При создании логотипа конференции использован рисунок из книги С.М. Флейшмана «Селевые потоки» (Москва: Географгиз, 1951, с. 51).
Conference logo is based on a figure from S.M. Fleishman's book on Debris Flows (Moscow: Geografgiz, 1951, p. 51).

ISBN 978-9941-26-283-8

The mud/debris flow of the Stava (Italy) tailings dams break

R. Genevois[1], P.R. Tecca[2]

[1]*Department of Geosciences, University of Padova, Padova, Italy, rinaldo.genevois@unipd.it*

[2]*Research Institute for Geo Hydrological Protection, National Research Council (CNR-IRPI), Padova, Italy, pia.tecca@irpi.cnr.it*

The wastes resulting from the chemical and mechanical processes of mining extraction (tailings) are mostly accumulated in basins retained by a dam that usually, after the construction of the starter dam, are raised sequentially as the impoundment fills with an upstream or downstream or centerline method. Tailing dams are particularly vulnerable to failure mainly due to: (i) poor quality of local material used for the starter dam; (ii) dam construction with solid material mixed with high quantity of water; (iii) lack of specific design criteria; (iv) lack of extensive and continuous monitoring; (v) high cost of remediation works, after the closure of mining activities. The assessment of tailings facilities has mainly concentrated on the stability of tailings dams, while relatively few studies have investigated the flow of tailings released from a dam failure due to the its complex rheological behavior. Furthermore, as many changes in the rheological values along the run-out path have been observed, different interpretations of the flow behavior exist. On July 19, 1985, a fluorite tailings dam failed at Stava, Trento, Italy. About 180,000 m3 of tailings flowed 4.2 km downstream killing 268 people and destroying 62 buildings. The tailings dams consisted of two partially overlapped basins built on a slope. The failure started at 12.22:55 with the collapse of the up-slope basin that caused the overtopping and subsequent collapse of the lower basin. The resulting slurry wave travelled along the Stava Creek reaching a speed as high as 100 km/h, until it reached the Avisio River. Different Authors [e.g.: R.J. Chandler and G. Tosatti, 1995; R. Genevois ant P.R. Tecca, 1993] concluded that the dams were constructed with an unacceptably low factor of safety and that the failure probably was triggered by a blocked decant pipe located within the tailings. In particular, the main causes of instability were found to be: (i) the under-consolidation state of the deposited material; (ii) the spreading of the upper dam on the lower basin; (iii) the excessive height and slope of the dams; (iv) the use of the upstream method, which is the cheapest, but also the most dangerous one; (v) the wrong installation of the drainage pipes. This paper, after a short history of the dams, will present a geotechnical analysis of the dam's failure and an analysis of the flow along the Stava valley.

tailings ponds, dam failure, mud flow, finite element analysis

Грязекаменный поток при прорыве дамбы хвостохранилища Валь-ди-Ставе (Италия)

Р. Женевуа[1], П.Р. Текка[2]

[1]*Департамент наук о Земле, Падуанский университет, Падуя, Италия, rinaldo.genevois@unipd.it*

[2]*Исследовательский институт по гидрогеологической защите, Национальный совет по науке, Падуя, Италия, pia.tecca@irpi.cnr.it*

Отходы, образующиеся в хвостохранилищах в результате химических и механических процессов добычи полезных ископаемых, в основном накапливаются в бассейнах, удерживаемых плотиной, которая обычно после строительства стартерной плотины постепенно поднимается, по мере заполнения водохранилища.

Хвостохранилища особенно уязвимы к прорыву дамб, главным образом из-за: (i) низкого качества местного материала, используемого для главной плотина; (ii) строительства плотины из твердого материала, смешанного с большим количеством воды; (iii) отсутствия конкретных критериев проектирования; (iv) отсутствия масштабного и непрерывного мониторинга; (v) высокой стоимости восстановительных работ после окончания горнодобывающей деятельности. Оценка хвостохранилищ в основном была сосредоточена на их устойчивости, в то время как относительно небольшое количество исследований было посвящено изучению потоков, образующихся вследствие разрушения плотин. Причина этого в сложности реологических свойств данных потоков. Кроме того, вследствие значительных изменений реологических характеристик потока, обнаруженных в результате наблюдений, существуют разные варианты интерпретации поведения данных потоков. 19 июля 1985 года в Тренто, Италия, провалилась плотина флюоритового хвостохранилища валь-ди-Ставе. Около 180 000 м^3 материала было вынесено на 4.2 км вниз по течению, что привело к гибели 268 человек и уничтожению 62 зданий. Плотины хвостохранилищ состояли из двух частично перекрытых бассейнов, построенных на склоне. Разрушение дамбы началось в 12.22:55 с прорыва верхнего бассейна, что вызвало переполнение и последующий прорыв нижнего. Образовавшаяся в результате волна шлама пролетела вдоль реки Ставы, достигая скорости до 100 км/ч, пока не достигла реки Авизио. Различные авторы, например, [*Chandler and Tosatti, 1995; Genevois and Tecca, 1993*] пришли к выводу, что плотины были сконструированы с неприемлемо низким коэффициентом безопасности и что прорыв, вероятно, был вызван блокированием трубы, расположенной в хвостохранилищах. В частности, были обнаружены основные причины нестабильности: (i) состояние консолидации депонированного материала; (ii) распространение верхней плотины на нижнем бассейне; (iii) чрезмерная высота и уклон плотин; (iv) использование метода восходящего потока, который является самым дешевым, но также и самым опасным; (v) неправильная установка дренажных труб. Эта статья после короткого описания истории данного события содержит геотехнический анализ разрушения плотин и анализ потока вдоль долины Ставы.

хвостохранилища, разрушение дамбы, грязевой поток, метод конечных элементов

Introduction

Tailings are mixtures of crushed rock and processing fluids from mining operations that remain after the extraction of metals, minerals, mineral fuels or coal from the mine resource [*Kossoff et al. 2014*]. These wastes are commonly deposited as slurry behind earthen dams, built with steep slopes using the coarse fraction of the tailings. Tailings dams are often raised in upstream/downstream valleys, or in ring impoundments. These containment facilities are vulnerable to failure because of the following reasons [*Rico et al., 2008a*]: (i) dam construction with residual materials from the mining operations; (ii) sequential dam raise along with an increase in effluents; (iii) lack of regulations on specific design criteria; and (iv) high maintenance cost also after the closure of mining activities.

Tailings dams have a very long history of flow failures; in the last 50 years, major failures causing fatalities and severe properties damages are known to have taken place in Buffalo Creek (USA), 1972; Bafokeng (South Africa), 1974; Taoshi (China), 2008; Karamken (Russia), 2009 and Kolòntar (Hungary), 2010, (WUP, 2018).

Although the major percentage of failures is related to natural hazards, in particular to meteorological causes [*Rico et al., 2008b*], failures due to poor management accounted for 30% [*Azam S. and Li Q., 2010*]. Many flow failures are associated with high water pools stored on tailings, which might cause: (i) breaching of containment embankment, resulting in release of water and tailings erosion; (ii) loss of containment embankment, resulting in rapid loss of lateral containment of tailings combined with excess pore pressures in tailings mass, liquefying the tailings mass.

This paper presents a well-documented case of the failure of two tailings dams of a fluorite mine, occurred in 1985, at Stava (North-Eastern Italy) (Fig. 1). The failure produced a catastrophic flow slide and consequent mud flow, which wiped out or buried two villages and claimed 268 lives, completely destroying 3 hotels, 53 homes, and six industrial buildings; 8 bridges were demolished and 9 buildings were seriously damaged.

Previous contributes dealing with the Stava debris flow include: description of the event [*Berti et al., 1988*]; failure mechanism [*Genevois and Tecca, 1993; Berti et al., 1997; Chandler and Tosatti 1995*] and flow kinematics [*Takahashi, 1991; Pirulli et al., 2017*].

This paper, after a short history of the dams, will show the two stages of the event, the earlier flow slide and the consequent debris/mud flow, and the geotechnical analyses of both the dams failure and the flow along the Stava valley.

Fig. 1. Aerial view of the area impacted by the mudflow and location of the tailing dams (Aerial photo: Permit of the general staff of the Italian Air Force No. 01-120 and No. 01-121 of March 22, 1995)

Chronicle of the event

On July 19, 1985 at 12.22.55, the upper dam collapsed first, slumping in the subjacent one and triggering the collapse of the lower dam. The resulting mudflow caused one of the worst industrial catastrophes in the world, second in Italy only to the Vajont tragedy, producing 155 million Euros in damage. A volume of 185.000 cubic metres of silt, sand and water were released toward the village of Stava and, from here into the Stava valley and at a speed up to

37 m/s (estimated from the seismogram recorded at the nearby Cavalese station, 4.1 km from the tailings dams), with an estimated volumetric solids concentration of 0.48 [*Takahashi*, *2007*]. The flow reached the village after 100 seconds, crashing through the buildings, the flow then continued for three minutes until it reached the Avisio River, 4.2 km away, engulfing and destroying everything in its path. Eventually, a layer of mud, between 20 and 40 centimetres thick, covered an overall 435,000 square meters over a 4.2 km route.

Characteristics and development of the tailing dams

The Prestavel mine had been in operation since the 16th century [*Perna, 1964*] for exploiting argentiferous galena. In 1934 mining at Prestavel was redirected to the extraction of fluorite. To isolate and to concentrate the fluorite, the Prestavel mine in 1961 shifted from the simple gravimetric procedure to the more effective flotation-process, where a mixture of water, rocks and foaming agents are used to extract the fluorite from the rock debris.

For this purpose, two basins were constructed on a small tributary of the Stava Creek, at an elevation ranging from 1330 to 1380 m a.s.l.., on a slope between 12° and 16°. The lower basin was located about 120 m above the Stava valley floor, in a distance of 800 m to the small village of Stava. Fig. 2 shows the aerial view of the two basins photographed in September 1982.

Fig. 2. Aerial view of the two tailings dams in 1980 [*Archivio multimediale Fondazione Stava 1985 Onlus. http://multimedia.stava1985.it/search.html*]

The impoundments were founded on fluvio-glacial deposits covering a marly-arenaceous formation. The local geological features have an important significance because of the different permeability of the formations and the consequent possible existence of confined aquifers. The lower dam was raised on natural ground using the "upstream method": centreline of the embankment moved upstream, in relation to the starter dam, so that the upstream wall was built on the tailings beach. The upper dam was initially raised using the "centreline method" (embankment crest shifted upwards in the same position, in relation to the starter dam), so that, as the dam grew higher, its sandy front rested partly on the lower pond silty sediments (Fig. 3); from 1975 the upper dam was raised using the "upstream method".

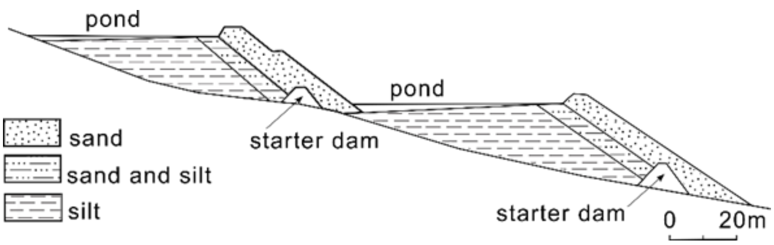

Fig. 3. Schematic cross section of the tailings dams

Two systems of tailings slurry disposal were employed: on-dam cycloning and central cycloning [*USEPA, 1994*]. A pool of clarified water accumulates upstream from the tailings sand beach and the dam crest was formed by cycloned sands.

Table 1 shows the development history of the two tailings dams and the sequence of the most important events which led to the failure.

Table 1. History of the Prestavel tailings basins

Time	Tailings basins
1961	First lower basin constructed; starter dam of gravelly natural soil, founded on natural ground reinforced by concrete soil-nailing; 9 m high and gradient 40°
Late 60’	Lower dam reached a height of 26 m [upstream method] and gradient 32°
1979	Second upper basin constructed; starter dam of gravelly compacted natural soil, no reinforcement of foundation soil; 5 m high
Early 70’	Upper dam reached a height of 10 m [centerline method] and gradient 39°
1975	Turning to upstream method, upper dam reached a height of 19 m; construction of a berm 4 m wide providing the dam a mean gradient 35°
1978	Upper dam reached a height of 26 m and gradient 39°; high water levels in the basins
1980-1982	Basins not used for different enriching fluorite method
1982	Floatation processing resumes; upper basin used; Upper dam reached a height of 28 m
Jan 1985	Small slump on the right side of the Upper dam [blockage by freezing of the decant pipe and consequent leakage]
Early June 1985	Sink hole 30 m wide and 4 m deep is formed in the lower basin (breakage of its decant pipe)
July 15 1985	Decant pipes restored; lower basin refilled; Upper dam reached a height of 30 m
July 19 1985	Tailings dams fail

The geotechnical properties of the tailings and of the embankment soils were investigated after the disaster by means of laboratory and field tests. Grain size distributions clearly differentiated the embankments materials, defined as silty-sands (PI between 4 and 7), from the sediment of the impoundments, defined as clayey silts (PI between 10 and 20).

In order to calculate the shear strength of soils, laboratory triaxial and shear box tests (drained and undrained conditions) and field tests (SPT and CPT) were carried out both on undisturbed and recompacted remoulded samples taken from the ponds and dams remnants.

The sandy tailings were found in a medium dense state, showing in situ resistances slightly increasing with depth, and average relative densities decreasing from 50% to 40% at depths greater than 6 m. The drained and effective angles of shear strength were estimated ranging between 37°-51° on undisturbed samples, and between 29°-40° on the recompacted ones, quite close to the gradient of the outer slope (34° and 39°).

The shear strength of the silty tailings showed values of the undrained cohesion ranging from 3 to 60 kPa, with a ratio s_u/σ'_{v0} ranging from 0.15 to 0.22 (s_u measured strength; σ'_{v0} effective vertical stress).

Consolidation tests evaluated compression indexes from 0.15 -0.28 for undisturbed samples and from 0.20-0.37 for remoulded samples, characterizing these sediments with an average degree of consolidation of 50%, with minimum values of 20-22%. The coefficient of consolidation, calculated for vertical stress of 200 kPa, showed values generally equal to 2x10-2 cm^2/s.

The dams failure analysis

While many Authors have analysed the dynamics of the flow all along the valley [*e.g., Takahashi, 1991; Pirulli et al., 2017*], not too much attention has been given to the initial failure of the dams, probably as a consequence of the insufficient knowledge of the different material geotechnical characteristics and space distribution, besides the uncertainty and debatable of the choice between total or effective stress analysis.

The causes of the Stava dams failure are generally attributed to the chronic instability of the embankments, mainly consequence, inter alia of the incomplete consolidation of the silty slime and the excessive height and slope of the embankments. Among the others, *Genevois and Tecca* [1993].

Considering a range of possible piezometric surfaces within the sandy shell, *Genevois and Tecca* [1993] carried out stability analyses using a two-dimensional non-linear finite difference code [*FLAC, Itasca Consulting Group 1992*]; the Drucker-Prager plasticity model was implemented on a simplified geometry of the tailings dam (Fig. 4), considering a range of possible piezometric surfaces within the outer sandy shell. The input geotechnical parameters are showed in Table 2.

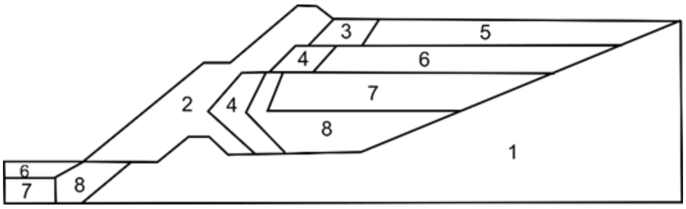

Fig 4. Geotechnical model of the 1985 Upper dam. 1- natural soil; 2- sands; 3- very soft alternating soils; 4- soft to medium alternating soils; 5- unconsolidated slimes; 6- very soft slimes; 7- soft slimes; 8- medium consolidated slimes

Table 2. Geotechnical parameters

Soil	**Γ (kN/m^3)**	**ϕ' (°)**	**c_u (kPa)**	***E* (MPa)**	***v***
1	20.6	40	-	150	0.25
2	18.6	42	-	35	0.30
3	17.2	36	-	15	0.35
4	18.1	37	-	25	0.35
5	13.7	-	7	3	0.35
6	16.2	-	15	6	0.35
7	17.7	-	25	9	0.35
8	18.6	-	35	12	0.35

γ - specific weight; ϕ' - friction angle; c_u undrained cohesion; *E* - Young modulus; *v* - Poisson coefficient. Material numbers are referred to Fig. 4.

The results of the analyses showed that the stability of the upper dam is mainly influenced by the dam height and by the position of the phreatic surface within the sandy shall and.

The safety factor displayed an initial increase due to the progressive consolidation of the slimes and a significant decrease after 1982, when the instability condition was reached for high piezometric levels.

The influence of the height increase of the upper dam was evaluated implementing the *Lade* [1992] procedure, identifying a region of potential instability. A local zone of instability already existed in 1975, and it extended more and more upwards and inwards as the dam height increased, eventually engaging the silty sands alternating layers and part of the silty tailings (Fig. 5).

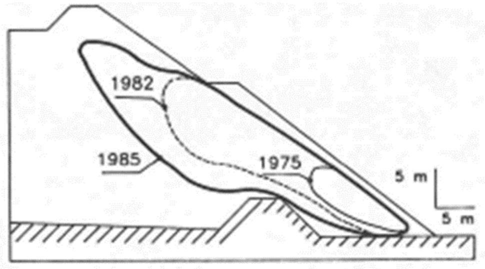

Fig. 5. Progressive extension of the instability zone during the upper dam building

The upper dam, however, was stable as long as drained conditions were secured: any pore pressure build up would have resulted into the enlargement of the unstable region, the engagement of progressively larger volumes of unstable tailings and finally into the dams failure by static liquefaction.

Event analysis: the flow slide and the mud/debris flow

Aerial photo interpretation, eyewitness accounts, and field observations indicate the most probable temporal sequence of the failure: (i) collapse of the sandy shell of the upper dam onto the silty tailings of the lower basin; (ii) liquefaction of the silty tailings of both the lower basin (undrained loading) and the upper basin (undrained unloading); (iii) flow of the sandy tailings down to the valley.

The Stava event has been subdivided into two different processes (Fig. 6): a flow slide from the tailing dams to the Stava village, where significant depositional processes took place, and a mud/debris flow along the Stava valley, where only erosional phenomena occasionally occurred [*Berti et al. 1997*]. The distinction in two processes is also confirmed by the interpretation of the seismogram recorded at Cavalese, 4.1 km from the Prestavel basins.

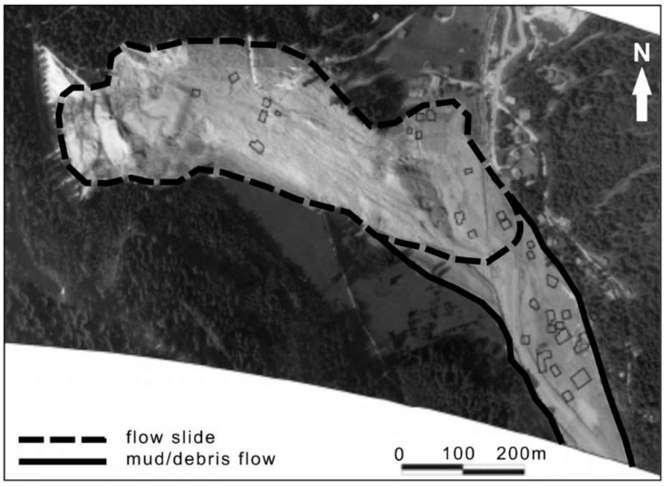

Fig. 6. The flow slide area with remnants of the dams and the upper part of the mud/debris flow a few hours after the disaster [photo Aeron. Mil., conc. S.M.A. no. 623, 19 July 1985].

The main phases composing the whole Stava event are visible in the time domain of the induced seismogram (Fig. 7). It lasted approximately 600 s, showing a magnitude between 2 and 3 in the Richter Scale. Amplitudes were rather low, showing peaks mostly lower than 1.5 μm/s with peak values up to 2 μm/s.

Different interpretations of the seismogram have been performed using different approaches [e.g. *Takahashi 1991; Pirulli et al., 2017*].

Our analysis, on the basis of both amplitudes and frequencies, identifies 6 different phases of the whole event, punctuated in time by a sequence of events, displayed in Table 2.

The phase (1), characterized by increasing amplitudes of the seismic wave, lasts about 60 seconds and corresponds to the upper dams failure and lower dam collapse. In phase (2), characterized by amplitudes roughly homogeneous for about 100 s, mean velocity is about 6.0 m/s. The peak amplitude registered at 12:24:50 is related to the impact with the buildings closest to the lower dam.

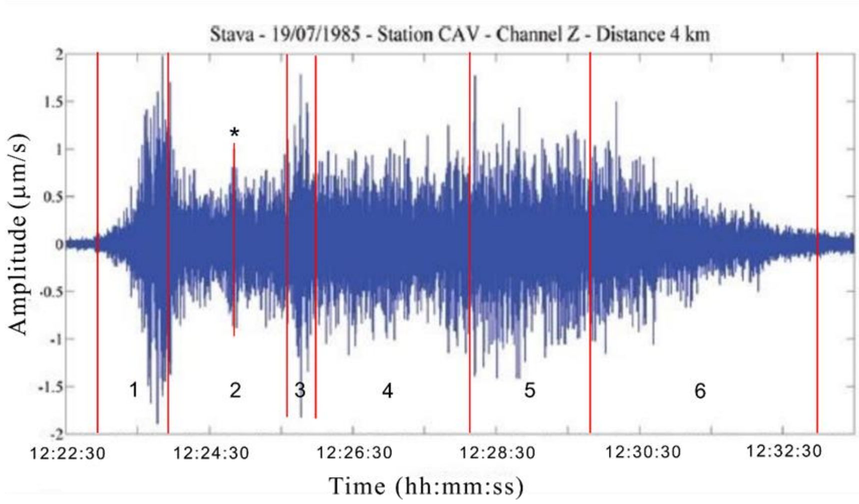

Fig. 7. Seismogram of the Stava event. Numbers are referred to the six distinct phases of the event indicated in Table 3.

Table 3. Sequence of events composing the Stava disaster

Phase	Time interval [hh:mm:ss]	Event	Process	Partial distance [m]	Mean velocity [m/s]
1	12:22:55-12:23:55	Upper and lower basins collapse	Dams failure	–	–
2	12:23:55 - 12:25:35	Slide path to upper Stava houses	Flow slide	600	6.0
*	12:24:50	Impact to buildings closest to the dams	Flow slide		
3	12:25:35-12:26:00	Wrecking of Stava Village	Mud/debris flow	270	10.8
4	12:26:00-12:28:10	Propagation along Stava valley to the Roman bridge in Tesero	Mud/debris flow	2950	22.7
5	12:28:10-12:29:50	Propagation from the Roman bridge to the Avisio River	Mud/debris flow	480	4.8
6	12:29:50-12:33:00	Deposition in the Avisio River valley	Deposition	–	–

* - single event

In phase (3), lasting about 25 s, the emerging peaks at 12:25:35 correspond to the impact and total wrecking to Stava village; flow velocity increased up to 10.8 m/s. The next phases (4) and (5), characterized by greater amplitude roughly homogeneous, correspond to the propagation of the mass along the Stava valley. In phase (4) mean velocity reached 22.7 m/s for about 130 s until the impact to the Roman bridge of Tesero at 12:28:10; in phase (5), lasting 110 s, the flow reached the Avisio River and mean velocity falls to 4.8 m/s. In phase (6) the amplitudes drop, indicating the deceleration of the mass and eventually the deposition of the material in the Avisio valley.

The analysis displays a significant change of the velocities observed all along the flow path.

The strong and fast increase of the mean velocity in phases (2), (3) and (4) has been interpreted as a variation of the flowing material characteristics. The collapsed material is mostly made by slightly to medium plastic silts (the impoundments material) and by nonplastic sands (the dam material).

Based on the Classification of Landslides of the Flow Type [*Hungr et al., 2001*], the initial process, composed by phases (1) and (2), may be classified as a flow slide of liquefiable silts and sands. The flow slide is characterized by medium to high mean velocity due to the high pore pressures induced by the previous undrained loading and unloading: this material accumulated at the end of the slope in a tongue-like form at the Stava village (see Fig. 6).

Downstream of the village, during the propagation phases (4) and (5), the mixture, mainly composed by sands and secondarily by silts, was channelled into the Stava valley, and the mass movement turned into an extremely rapid mud/debris flow (see Fig. 6).

Conclusions

The failure of the Stava basins has been here reconsidered as regards mainly the dynamics of the flow. As matter of facts, different interpretations of the flow dynamics exist [e.g. *Takahashi 1991; Berti et al. 1997; Pirulli et al. 2017*], mainly depending on the rheological behavior attributed to the flowing mass, but only Berti et al in 1997 considered the event as composed by two different processes: an initial flow slide and a following mud/debris flow.

The careful analysis of the seismic record indicates a sudden acceleration of the flowing mass when it entered the Stava valley, differentiating the previous flow of mainly silty materials, identified as a flow slide, from the following faster flow of mainly sandy material, considered a mud/debris flow, as confirmed also by the field surveys after the disaster.

As regards the initial failure of the upper dam, the causes should be referred in general to the poor engineering of the construction and, in particular, to the raising of the upper dam with a steep downwards slope. As a conclusion, the dam was only marginal stable and it would have in any case collapsed.

References

Archivio multimediale Fondazione Stava 1985 Onlus. http://multimedia.stava1985.it/search.html. Last access April 2018.

Azam S., Li Q. (2010). Tailings Dam Failures: A Review of the Last One Hundred Years. Geotechnical News, 50-54.

Berti M., Genevois R., Tecca P.R. (1997). The 1985 flow slide and debris flow at Stava (Italy). In 1st International Conference on “Debris Flow Hazard Mitigation: Mechanics, Prediction and Assessment”, 7-9 August 1997, San Francisco (Cal.), ed. Chen Cheng-Iung, 309–321. American Society of Civil Engineers. New York.

Chandler R.L., Tosatti G. (1995). The Stava tailings dams failure, Italy, July 1985. Proceedings of the Institution of Civil Engineers: Geotechnical Engineering, 133, 67–79.

Genevois R., Tecca P.R. (1993). The tailings dams of Stava (northern Italy): an analysis of the disaster. In Environmental Management Geo-water and Engineering Aspects, ed. R.N. Chowdhury and M. Sivakumar, 23–36. Balkema, Rotterdam.

Hungr O., Evans S., Bovis M., Hutchinson J.N. (2001). Review of the classification of landslides of the flow type. Environmental & Engineering Geoscience, 7: 221-238. 10.2113/gseegeosci.7.3.221.

Itasca (2012). FLAC: Fast Lagrangian Analysis of Continua. Version 7.0. Itasca Consulting Group, Inc., Minneapolis, Minn.

Kossoff D., Dubbin W.E., Alfredsson A., Edwards S.J., Macklin M.G., Hudson-Edwards K.A. (2014). Mine tailing dams: characteristics, failure, environmental impact, and remediation. Applied Geochemistry, 51: 229–245.

Lade P. (1992). Static Instability and Liquefaction of Loose Fine Sandy Slopes. Journal of Geotechnical Engineering, 118(1), 51-71.

Perna G. (1964). Fluorite. L’Industria Mineraria nel Trentino-Alto Adige. Economia Trentina, XIII: 66–68 (in Italian).

Rico M., Benito G., Salgueiro A.R., Dìez-Herrero A., Pereira H.G (2008a). Reported tailings dam failures. A review of the European incidents in the worldwide context. Journal of Hazardous Materials, 152: 846–852.

Rico M., Benito G., Dìez-Herrero A. (2008b). Floods from tailings dam failures. Journal of Hazardous Materials, 154: 79–87.

Pirulli M., Barbero M., Marchelli M., Scavia C. (2017). The failure of the Stava Valley tailings dams (Northern Italy): numerical analysis of the flow dynamics and rheological properties. Geoenvironmental Disasters, 4:3. doi 10.1186/s40677-016-0066-5.

Takahashi T. (1991). Debris flows., IAHR Monograph, Balkema, Rotterdam.

Takahashi T. (2007). Debris flows: Mechanics, prediction and countermeasures. Monograph, Balkema, Rotterdam.

USEPA. Design and Evaluation of Tailings Dams. Technical Report EPA 530-R-94-038, US Environmental Protection Agency, Washington, available at: https://archive.epa.gov/epawaste/nonhaz/industrial/special/web/pdf/tailings.pdf. Last access April 2018.

WUP. Wise Uranium Project – Chronology of major tailings dam failures [from 1960], available at: http://www.wise-uranium.org/mdaf.html. Last access August 2018.